WISC

UNIVERSITY OF WISCONSIN • MADISON, WISCONSIN

PLASMA PHYSICS

44
10-17-96 JSS (1)

INCREASED CONFINEMENT AND BETA BY INDUCTIVE POLOIDAL CURRENT DRIVE IN THE RFP

J.S. Sarff, N.E. Lanier, S.C. Prager, and M.R. Stoneking

DOE/ER/54345-283 October 1996

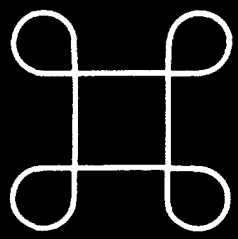

ONSIN

NOTICE

Printed in the United States of America
Available from
National Technical Information Service
U.S. Department of Commerce
5285 Port Royal Road
Springfield, VA 22161

NTIS Price codes
Printed copy: A02
Microfiche copy: A01

Increased Confinement and Beta by Inductive Poloidal Current Drive in the RFP

J. S. Sarff, N. E. Lanier, S. C. Prager, and M. R. Stoneking

University of Wisconsin, Madison, WI 53706

Progress in understanding magnetic-fluctuation-induced transport in the reversed field pinch (RFP) has led to the idea of current profile control to reduce fluctuations and transport. With the addition of inductive poloidal current drive in the Madison Symmetric Torus (MST), the magnetic fluctuation amplitude is halved, leading to a four- to five-fold increase in the energy confinement time to τ_E~5 ms as a result of both decreased plasma resistance and increased stored thermal energy. The record low fluctuation amplitude coincides with a record high electron temperature of ~600 eV (for MST), and beta $\beta = 2\mu_o \langle p \rangle / B(a)^2$ increases from 6% to 8% compared with conventional MST RFP plasmas. Other improvements include increased particle confinement and impurity reduction.

PACS Numbers: 52.55.Hc, 52.35.Py, 52.25.Gj, 52.25.Fi

A growing understanding of the turbulence in reversed field pinch (RFP) plasmas has inspired recent proposals to reduce magnetic fluctuations and associated transport by the application of current density profile control. The majority of the energy loss in an RFP plasma occurs through transport in a stochastic magnetic field generated by magnetic fluctuations. Most of these fluctuations result from several poloidal mode number m=1, toroidal mode number n~$2R/a$, magnetohydrodynamic (MHD) tearing instabilities[1] resonant in the core of the plasma and driven by the current density gradient. Direct measurements of the magnetic-fluctuation-induced particle[2] and heat[3] losses in the Madison Symmetric Torus (MST) identify large transport associated with these fluctuations. In other RFP experiments,[4] the estimated magnetic-fluctuation-induced heat flux can account for the observed volume averaged heat flux. The fluxes measured in MST agree with expectations[5] for stochastic magnetic field diffusion, except the electron heat loss in the outer region of the plasma occurs at the ion rate, perhaps as a result of self-consistency associated with ambipolar constraints on the particle transport.[6] Since tearing instability results from the current density gradient, the proposals for current profile control employ auxiliary electrostatic,[7] rf,[8,9] or neutral beam[10] current drive in the outer region of the plasma. In a conventional RFP plasma, the tearing fluctuations drive current in the outer region through a $\langle \tilde{\mathbf{V}} \times \tilde{\mathbf{B}} \rangle$ motional emf or "dynamo" effect,[11] establishing a self-consistent current profile. The auxiliary current drive, aimed to reduce the current density gradient, may be viewed as a replacement for dynamo current drive, reducing the fluctuations otherwise essential to sustain the RFP magnetic equilibrium.

In this Letter we describe the observation of reduced magnetic fluctuations and transport resulting from inductive poloidal current drive in an RFP. With poloidal current drive, the magnetic fluctuation amplitude reaches a

record low value (for MST and probably for any RFP). The global energy confinement time increases four- to five-fold as a result of both dramatically decreased plasma resistance and increased stored thermal energy. A record high (for MST) electron temperature ~600 eV is achieved, and the beta value increases from 6% to 8%. In conventional RFP operation, an inductive toroidal electric field drives the plasma current. With the addition of a poloidal component, the electric field parallel-to-**B** is increased in the outer region of the plasma (where the magnetic field is mostly poloidally directed) to facilitate current profile flattening for fluctuation suppression. Unlike the proposed electrostatic, rf, or neutral beam current drive, inductive poloidal current drive is inherently transient since it produces a changing toroidal flux in the plasma volume. The observed improvements last as long as poloidal current drive is present. We hereafter refer to this technique as pulsed poloidal current drive (PPCD).

The PPCD experiment is performed in MST,[12] a large reversed field pinch with major radius R=1.5 m, minor radius a=0.52 m, toroidal plasma current $I_\phi \leq 500$ kA, and beta $\beta = 2\mu_o \langle p \rangle / B(a)^2 \leq 10\%$. The waveforms of the toroidal and poloidal components of the electric field E_ϕ and E_θ (measured at the plasma surface), the toroidal current I_ϕ, the average toroidal magnetic field $\langle B_\phi \rangle = \Phi / \pi a^2$, and the toroidal field at the surface $B_\phi(a)$ during a PPCD experiment are shown in Fig. 1. The shaded region indicates the time during which PPCD is applied. In the first PPCD experiment,[13] the E_θ drive was a single, triangular shaped pulse. Figure 1 illustrates improved PPCD that provides a series of four smaller pulses. Improved PPCD drives poloidal current more uniformly throughout the PPCD phase and reduces the plasma-wall interaction since the peak E_θ amplitude of the four pulses is smaller. Also PPCD lasts longer, maintaining the beneficial effects observed in the first experiment for a longer period of time. Most importantly, improved PPCD leads to a greater

reduction in the magnetic fluctuation amplitude and an increase of the stored thermal energy, energy confinement, and beta. The sharp negative spikes in E_θ both before and after PPCD are associated with plasma-generated toroidal flux in spontaneous sawtooth (dynamo) events (Fig. 1d). The negative E_θ spikes represent the toroidal field magnet circuit's inductive back-reaction to dynamo flux generation within the plasma volume, and they oppose the dynamo-driven emf.[14] In contrast, PPCD is a controlled increase in the poloidal current through application of positive E_θ.

A new result of improved PPCD is the reduction of the magnetic fluctuation amplitude to a record low value. The spatial root-mean-square magnetic field fluctuation $\tilde{b}_{rms}$ measured in an improved PPCD discharge by a 32-station toroidal array of pickup coils on the plasma surface is shown in Fig. 2a, normalized to the equilibrium field strength $B(a)$. The dominant wavelengths that compose this fluctuation are m=1, n=6-10 modes, although the m=1, n=6 mode alone accounts for most of the fluctuation during PPCD. Before PPCD is applied, the fluctuation amplitude cycles with the sawtooth oscillation at a cycle-averaged amplitude of $\tilde{b}_{rms} / B(a) \approx 1.5\%$ typical of conventional RFP plasmas. PPCD suppresses sawtoothing, and the fluctuation amplitude first grows slowly and then decreases. Large sawteeth are suppressed in virtually all PPCD discharges, but the fluctuation amplitude in the first PPCD experiment[13] was held at the "between sawtooth crash" value. With improved PPCD, the fluctuation in some discharges (like that of Fig. 2) is reduced *below* the sawtooth cycle minimum value to a record low value $\tilde{b}_{rms} / B(a) \approx 0.8\%$. During these periods of very low fluctuation, the improvements in the plasma are most dramatic. The parallel electric field $E_\parallel = \mathbf{E} \cdot \mathbf{B} / B \approx E_\theta$ measured at the plasma surface is shown in Fig. 2c to emphasize the relationship of reduced magnetic fluctuation and poloidal current drive. While poloidal current is driven by

PPCD, the fluctuation amplitude is small. Although large sawteeth are suppressed by PPCD, a new type of smaller sawtooth phenomena[15] occurs during and immediately following PPCD. In Fig. 2c, the presence of these smaller sawteeth is evidenced through the negative $E_{\|}$ spike at $t \approx 16$ ms during PPCD and by the series of negative spikes that immediately follow PPCD. The transition of the fluctuation to its low value coincides with a small sawtooth in this and many improved PPCD plasmas. This is probably related to an abrupt, but modest, current profile adjustment associated with the small sawtooth crash, but the current drive provided by improved PPCD appears necessary as well. Periods of very low fluctuation are not observed when duplicating the original single pulse E_θ programming. The details of the current penetration into the plasma (and therefore the current profile modification) depend on the time variation of the applied surface electric field. Improved PPCD resulted from ongoing attempts to optimize the inductive electric field programming.

In addition to the magnetic field, many quantities show reduced fluctuations during PPCD. For example, the voltage φ_{float} in Fig. 2b from a floating Langmuir probe located at the edge of the plasma shows a reduction in fluctuations similar to that in Fig. 2a. (Note that Fig. 2a is a processed rms amplitude, and Fig. 2b is a "raw" measurement.) Electrostatic fluctuations have been identified as the most likely cause of particle transport in the edge of MST[16] and other RFP experiments. A possible connection between the reduction of magnetic fluctuations in the core and electrostatic fluctuations in the edge is an exciting prospect. Current profile control may have a more general consequence than the targeted reduction of global magnetic fluctuations.

The global energy confinement time τ_E increases during PPCD as a result of both increased stored thermal energy and decreased plasma resistance, *i.e.*, decreased Ohmic input power P_{Ohmic}. The shot-averaged[17] line density $\overline{n}_e$,

central electron pressure $n_{eo}kT_{eo}$, P_{Ohmic}, mean-squared magnetic fluctuation $\tilde{b}^2$, and H_α radiation for 100 PPCD plasmas with I_ϕ=340 kA are shown in Fig. 3. The shot-averages of the same quantities for 80 conventional RFP plasmas are overlaid for comparison. For purposes of comparison, the gas fueling was adjusted for matched density evolution. The central electron pressure is measured with a single point (time and space) Thomson scattering diagnostic, varied in time shot-by-shot. In estimating τ_E and β, the $n(T_e+T_i)$ radial profile is assumed to behave as $1-(r/a)^2$. (An 11-chord interferometer indicates the density profile is centrally peaked, but the temperature profiles are not measured.) The ion temperature measured by charge exchange is $T_i^{cx} \approx 0.5T_{eo}$ in conventional discharges at this density but remains roughly constant while T_{eo} increases by as much as 70% compared with conventional RFP plasmas. The Ohmic input power is derived from the measured total input power (Poynting flux) at the plasma surface by subtracting the rate of change of stored magnetic energy using equilibrium modeling (described in the next paragraph). The calculation includes input power from both E_ϕ and E_θ. The PPCD plasmas in this ensemble, chosen only for the same density, have increased τ_E from 1 ms to ~4 ms and increased β from 6% to ~7% compared with conventional RFP plasmas at a time near the end of PPCD (t≈17 ms). (The poloidal beta $\beta_\theta = 2\mu_o\langle p\rangle / B_\theta(a)^2$ increases from 6% to ~8%.) A smaller ensemble of 25 plasmas which exhibit the exceptionally low magnetic fluctuation level features illustrated in Fig. 2a have τ_E≈5 ms and β≈8% (β_θ≈9%). Table 1 summarizes improved PPCD confinement (coincident with the lowest magnetic fluctuation) in 340 kA plasmas. An MST record T_{eo} =615 eV was measured for similar improved PPCD plasmas at higher current I_ϕ=440 kA with $\bar{n} \sim 1\times10^{19}$ m^{-3}, although with smaller β≈7% but similar τ_E≈5 ms.

Although the increase in stored thermal energy is substantial, most of the increase in τ_E results from reduced P_{Ohmic}. Since PPCD is transient, accurate time-dependent equilibrium modeling is required to derive

$$P_{Ohmic} \equiv I_\phi V_\phi + I_\theta V_\theta - \frac{\partial}{\partial t}\int B^2 dV / 2\mu_o. \quad (1)$$

To evaluate the volume integrated (stored) magnetic energy, the three-parameter cylindrical equilibrium model[18]

$$\nabla \times \mathbf{B} = \lambda_o\left(1 - r^\alpha\right)\mathbf{B} + \left(\beta_o / 2B^2\right)\mathbf{B} \times \nabla p \quad (2)$$

is used to estimate $\mathbf{B}(r,t)$. The parallel-to-**B** current in Eq. 2 is specified by shape and amplitude parameters α and λ_o, and the perpendicular current is specified by the central beta parameter $\beta_o = 2\mu_o p_o / B_o^2$ and a pressure profile (assumed to be $p(r) \propto 1 - r^2$). The $\alpha(t)$, $\lambda_o(t)$, and $\beta_o(t)$ parameters are adjusted to match measured $I_\phi(t)$, $\langle B_\phi(t)\rangle$, $B_\phi(a,t)$, and $\beta(t)$. As a test of the model accuracy, the predicted "internal inductance" $l_i \equiv 2\int B_\theta^2 r dr / a^2 B_\theta(a)^2$ is compared with the internal inductance derived from the poloidal asymmetry in B_θ at the plasma surface $B_\theta(\theta) \approx \overline{B}_\theta(a)[1 + \frac{a}{R}\Lambda\cos\theta]$ measured by a 16-station poloidal array of magnetic sensors. The "asymmetry factor" Λ is related to l_i and β_θ by $\Lambda = l_i / 2 + \beta_\theta - 1$ for a circular cross-section plasma.[19] The comparison is shown in Fig. 4, where superscript "α" identifies equilibrium model results. The "total inductance" $L_{tot} / \mu_o R$, which includes the toroidal field contribution to the total magnetic energy, is also shown in Fig. 4 to illustrate that ~2/3 of the magnetic energy in an RFP is in the poloidal component (measured by l_i). The good agreement between l_i determined from Λ and l_i predicted by Eq. 2 bolsters confidence in the calculation of P_{Ohmic}. The energy confinement time (quoted above) is defined as

$$\tau_E \equiv \frac{\int \frac{3}{2} nk(T_e + T_i) dV}{P_{Ohmic} - \frac{\partial}{\partial t} \int \frac{3}{2} nk(T_e + T_i) dV} \quad . \tag{3}$$

Although thermal energy increasing during PPCD tends to decrease the denominator in Eq. 3, the impact of $\partial\beta / \partial t > 0$ on the equilibrium modeling increases P_{Ohmic} by a slightly larger amount, and the net effect is a $\leq$1 ms decrease in τ_E relative to a constant-β calculation.

The global particle confinement time τ_p also increases during PPCD. This is indicated by the decrease in H_α emission (ionization source) while n_e increases. Particle transport modeling estimates τ_p increases by a factor similar to the increase in τ_E. Also the plasma is cleaner, as evidenced by reductions in the total radiated power, including visible impurity line radiation and bremsstrahlung radiation. Higher energy soft x-ray radiation increases, consistent with the higher electron temperature. Although clean wall conditions are necessary to avoid impurity contamination associated with pulsed E_θ, improved PPCD does not require extreme conditioning measures. In the first PPCD experiment, boronization of the vacuum chamber was necessary to maintain impurity control.

In summary, inductive poloidal current drive decreases the amplitude of m=1 tearing fluctuations, suppresses their associated sawteeth, increases the plasma pressure, and increases the energy confinement time four- to five-fold in the MST RFP. The particle confinement time also increases. For the first time, the fluctuation amplitude falls below the "between sawtooth crash" level, and the confinement and beta improvements in the plasma are best during these periods of low magnetic fluctuation. Although PPCD does not eliminate tearing fluctuations, a clear correlation exists between improved confinement, poloidal current drive, and fluctuation reduction. If the transported energy loss scales like

$\chi \propto \tilde{B}_r^2$, as expected for diffusion in a stochastic magnetic field,[5] then the 50% reduction in the fluctuation amplitude predicts a four-fold decrease in energy transport. The observed four- to five-fold increase of the confinement time is consistent with this expectation.

The authors are grateful for the assistance of the MST group. This work was supported by the US DoE.

Table 1. MST confinement parameters with and without PPCD (compared at the same current and density near the end of the PPCD phase.)

	PPCD	Conventional RFP
Current, I_ϕ	340 kA	340 kA
Density, n_e	$1.0\times10^{19}\text{m}^{-3}$	$1.0\times10^{19}\text{m}^{-3}$
Temperature, T_{eo}	390 eV	230 eV
Poloidal Beta, β_θ	9%	6%
Input Power, P_{Ohmic}	1.3 MW	4.4 MW
Fluctuation, $\tilde{b}_{rms} / B(a)$	0.8%	1.5%
Confinement, τ_E	5 ms	1 ms

REFERENCES

[1]D.D. Schnack, D.C. Barnes, Z. Mikic, D.S. Harned, and E.J. Caramana, J. Comput. Phys. **70**, 330 (1987); also Y.L Ho and G.G. Craddock, Phys. Fluids B **3**, 721 (1991) and references therein.

[2]M.R. Stoneking, S.A. Hokin, S.C. Prager *et al.*, Phys. Rev. Lett. **73**, 549 (1994).

[3]G. Fiksel, S. C. Prager, W. Shen, and M. Stoneking, Phys. Rev. Lett. **72**, 1028 (1994).

[4]For example, I. H. Hutchinson *et al.*, Nucl. Fusion **24**, 59 (1984) and K. Hattori *et al.*, Phys. Fluids B **3**, 3111 (1991).

[5]J. D. Callen, Phys. Rev. Lett. **39**, 1540 (1977) and A. B. Rechester and M. N. Rosenbluth, Phys. Rev. Lett. **40**, 38 (1978).

[6]P.W. Terry, G. Fiksel, H. Ji *et al.*, Phys. Plasmas **3**, 1999 (1996).

[7]Y.L. Ho, Nucl. Fusion **31**, 341 (1991).

[8]E. Uchimoto, M. Cekic, R.W. Harvey et al., Phys. Plasmas **1**,3517 (1994).

[9]S. Shiina, Y. Kondoh, and H. Ishii, Nucl. Fusion **34**, 1473 (1994).

[10]K. Hattori, Y. Hirano, Y. Yagi, T. Shimada, and K. Hayase, Fusion Technol. **28**, 1619 (1995).

[11]H. Ji *et al.*, Phys. Plasmas **3**, 1935 (1996).

[12]R.N. Dexter, D.W. Kerst, T.H. Lovell, S.C. Prager, and J.C. Sprott, Fusion Technol. **19**, 131 (1991).

[13]J.S. Sarff, S.A. Hokin, H. Ji, S.C. Prager, C.R. Sovinec, Phys. Rev. Lett **72**, (1994).

[14]H. Ji, A.F. Almagri, S.C. Prager, and J.S. Sarff, Phys. Rev. Lett. **73**. 668 (1994).

[15]J.S. Sarff, A.F. Almagri, M. Cekic *et al.*, Phys. Plasmas **2**, 2440 (1995).

[16]T.D. Rempel, C.W. Spragins, S.C. Prager *et al.*, Phys. Rev. Lett. **67**, 1438 (1991).

[17]The PPCD programming for this ensemble is slightly different than for the single shot of Figs. 1 and 2.

[18]V. Antoni *et al.*, Nucl. Fusion **26**, 1711 (1986).

[19]J.P. Freidberg, Rev. Mod. Phys. **54**, 801 (1982).

FIGURE CAPTIONS

Fig. 1 Waveforms of the (a) surface toroidal electric field, (b) surface poloidal electric field, (c) the toroidal plasma current, and (d) the average and surface toroidal magnetic field.

Fig. 2 The (a) spatial root-mean-square magnetic fluctuation, (b) edge floating Langmuir probe voltage, and (c) the parallel electric field measured at the plasma surface during improved PPCD.

Fig. 3 Shot-averaged waveforms of (a) the central chord line density, (b) central electron pressure from Thomson scattering, (c) Ohmic input power, (d) mean-squared fluctuation amplitude, and (e) H_α radiation. The unbroken lines are for PPCD plasmas, and the broken lines are for conventional RFP plasmas.

Fig. 4 Normalized inductances for ensemble data of Fig. 3. Superscript "α" indicates equilibrium model predictions (Eq. 2). For better illustration of the time evolution, this comparison is shown for fixed β_θ=10%. (The temporal resolution of $\beta(t)$ is coarse.)

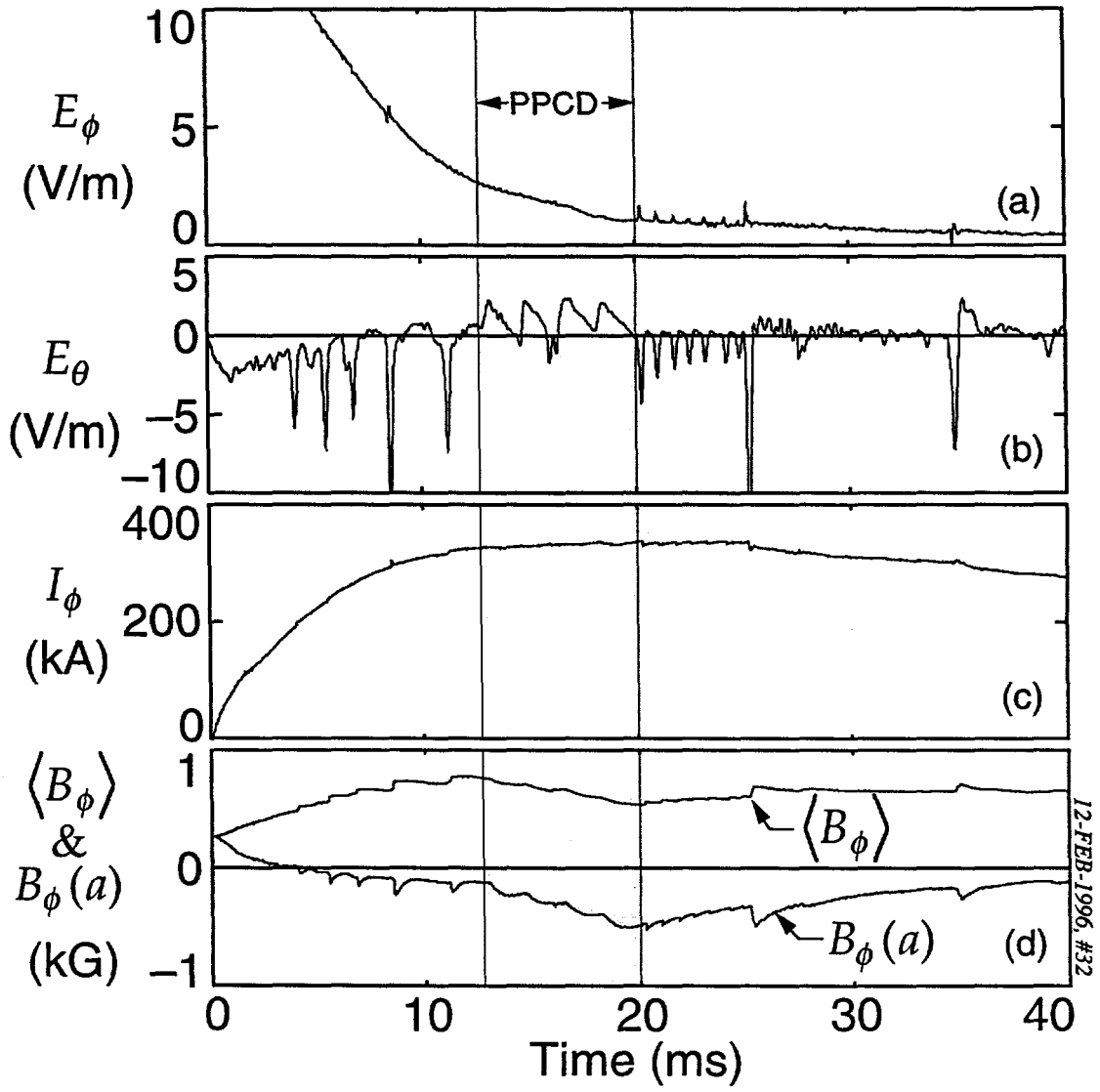

Fig. 1, *Reduction of Magnetic Fluctuations and Transport by Inductive Poloidal Current Drive,* J.S. Sarff et al.,

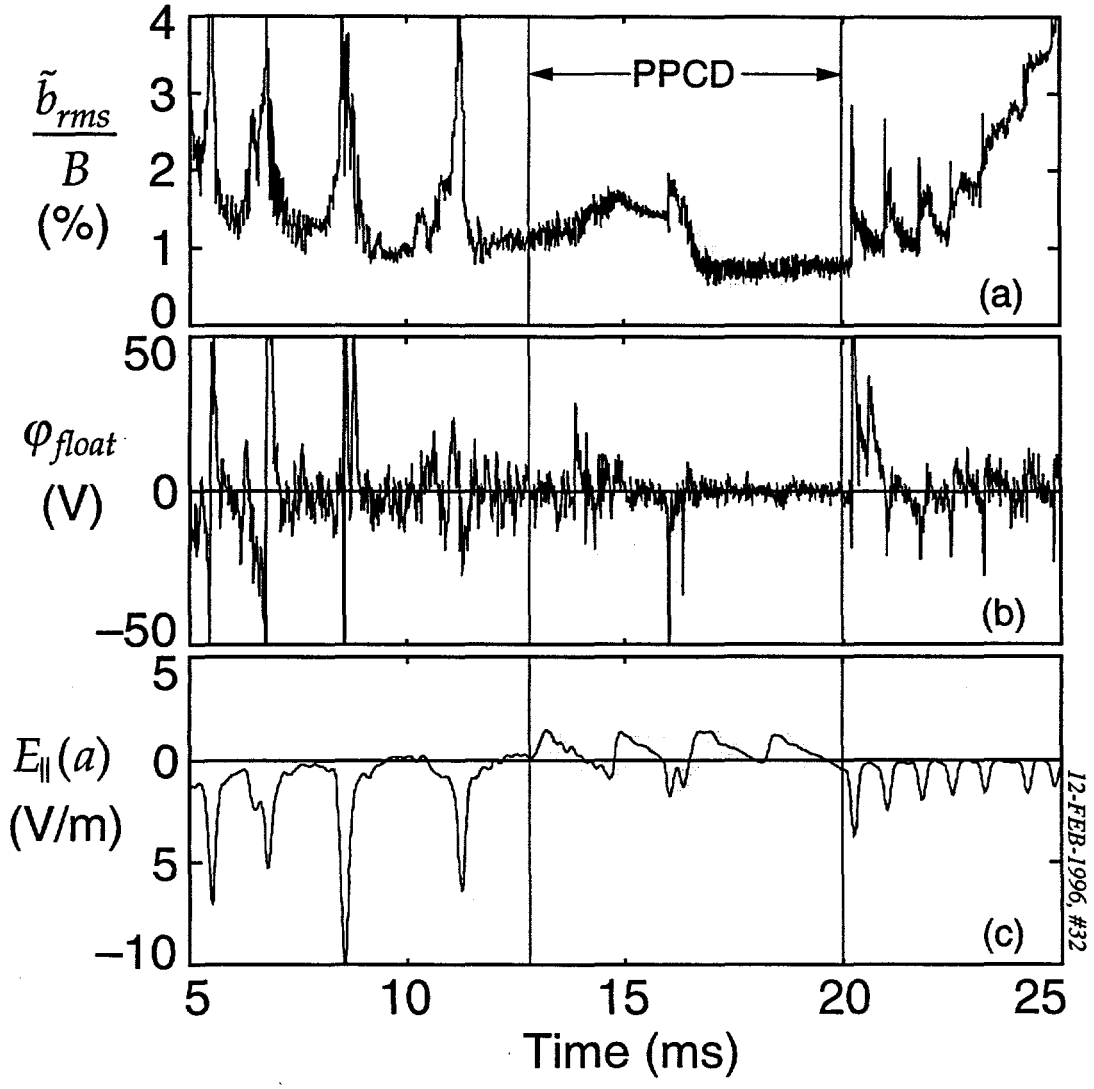

Fig. 2, *Reduction of Magnetic Fluctuations and Transport by Inductive Poloidal Current Drive,* J.S. Sarff et al.,

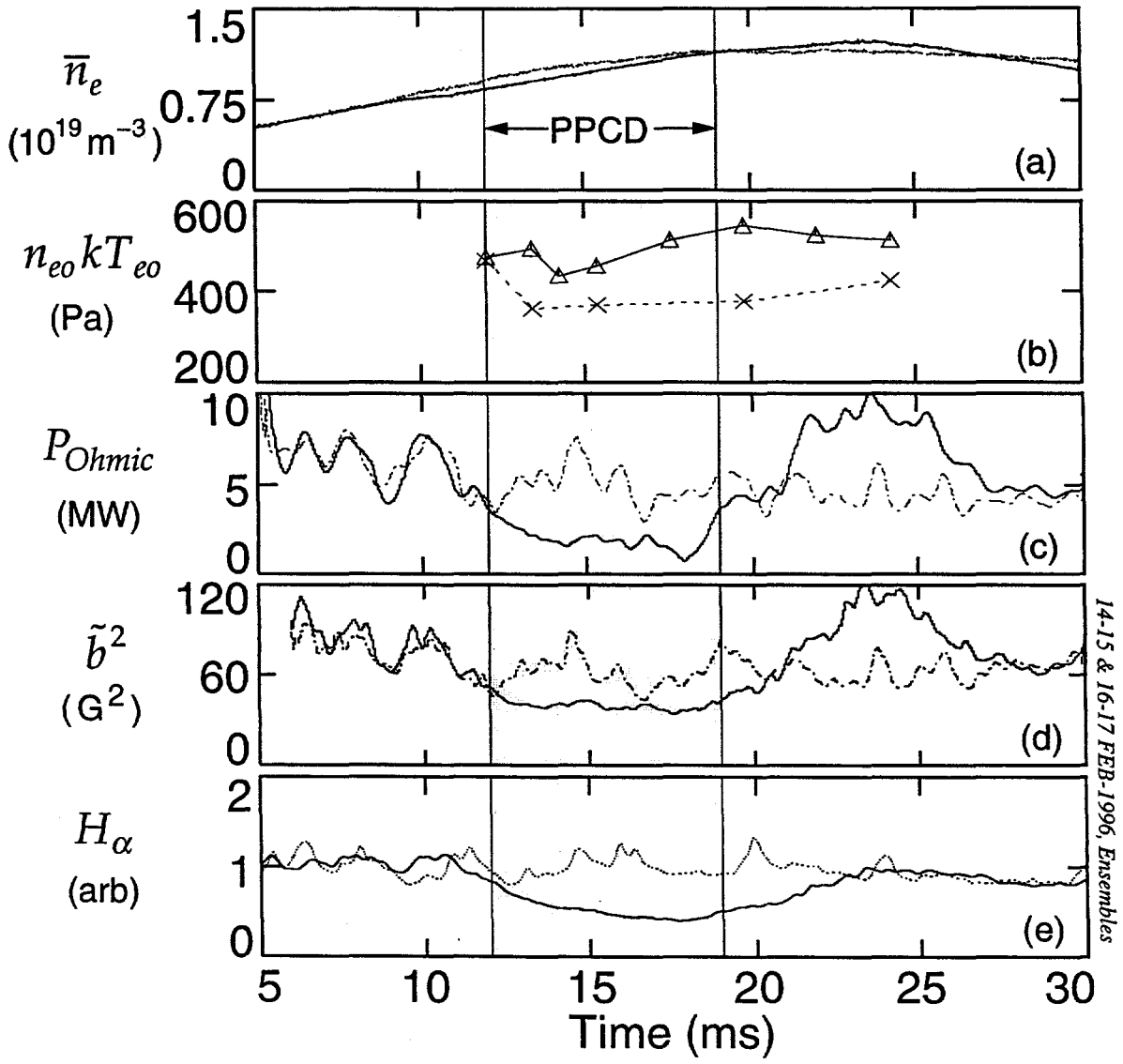

Fig. 3, *Reduction of Magnetic Fluctuations and Transport by Inductive Poloidal Current Drive,* J.S. Sarff et al.,

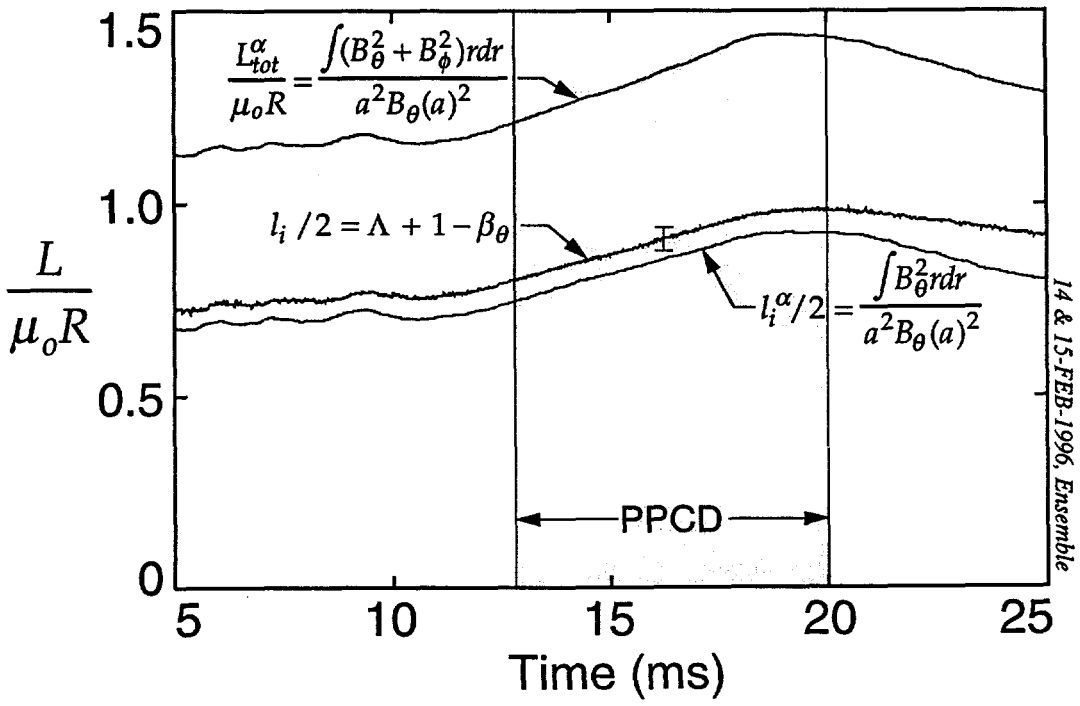

Fig. 4, *Reduction of Magnetic Fluctuations and Transport by Inductive Poloidal Current Drive,* J.S. Sarff et al.,

EXTERNAL DISTRIBUTION IN ADDITION TO UC-20

S.N. Rasband, Brigham Young University
R.A. Moyer, General Atomics
J.B. Taylor, Institute for Fusion Studies, The University of Texas at Austin
E. Uchimoto, University of Montana
F.W. Perkins, PPPL
O. Ishihara, Texas Technical University
M.A. Abdou, University of California, Los Angeles
R.W. Conn, University of California, Los Angeles
P.E. Vandenplas, Association Euratom-Etat Belge, Belgium
Centro Brasileiro de Pesquisas Firicas, Brazil
P. Sakanaka, Institute de Fisica-Unicamp, Brazil
Mme. Monique Bex, GANIL, France
J. Radet, CEN/CADARACHE, France
University of Ioannina, Greece
R. Andreani, Associazione EURATOM-ENEA sulla Fusione, Italy
Biblioteca, Istituto Gas Ionizzati, EURATON-ENEA-CNR Association, Italy
Plasma section, Energy Fundamentals Division Electrotechnical Laboratory, Japan
Y. Kondoh, Gunma University, Kiryu, Gunma, Japan
H. Toyama, University of Tokyo, Japan
Z. Yoshida. University of Tokyo, Japan
FOM-Instituut voor Plasmafysica "Rijnhuizen," The Netherlands
Z. Ning, Academia Sinica, Peoples Republic of China
P. Yang, Shandong University, Peoples Republic of China
S. Zhu, University of Science & Technology of China, People's Republic of China
I.N. Bogatu, Institute of Atomic Physics, Romania
M.J. Alport, University of Natal, Durban, South Africa
R. Storer, The Flinders University of South Australia, South Australia
B. Lehnert, Royal Institute of Technology, Sweden
Librarian, CRPP, Ecole Polytechnique Federale de Lausanne, Switzerland
B. Alper, Culham Laboratory, UK
A. Newton, UK

2 for Chicago Operations Office
5 for individuals in Washington Offices

INTERNAL DISTRIBUTION IN ADDITION TO UC-20
80 for local group and file